Tumblenauts: Towards a Bacteria-Inspired Robot Swarm for Intra-Vehicular Space Inspection

Sneha Ramshanker[1][0000−0002−1588−5505], Merihan Alhafnawi[1][0000−0003−1049−7877], Yushra Guffer[1][0009−0005−8259−0474], and Radhika Nagpal[1,2][0000−0001−9756−0167]

[1] Department of Mechanical and Aerospace Engineering, Princeton University, Princeton, NJ, USA
[2] Department of Computer Science, Princeton University, Princeton, NJ, USA
s.ramshanker@princeton.edu

Abstract. Tumblenauts are a swarm of minimalist, bacteria-inspired robots designed for collaborative inspection of pressurized microgravity habitats such as the International Space Station. Unlike current intra-vehicular robots that rely on complex, actuator-dense mechanisms for precise motion, the Tumblenauts use a stochastic run-and-tumble locomotion inspired by bacterial motility. This unique locomotion paradigm enables a simpler design, improves scalability, and greatly reduces actuation requirements, making the Tumblenauts among the smallest and least actuator-dense robots built for microgravity. In this paper, we present the design of the Tumblenaut, describe how it achieves run-and-tumble locomotion, and characterize its motion dynamics using Earth-based microgravity testbeds. Furthermore, using a data-driven simulation, we demonstrate how the Tumblenauts can perform a diverse set of inspection tasks by leveraging collective behavior. Specifically, we show that the swarm can collaboratively map environments, achieve directed navigation through a chemotaxis-inspired control mechanism, and make global inspection classification decisions by sharing information. As a new generation of space habitats is launched into orbit, we envision swarms of Tumblenauts run-and-tumbling within them, providing continuous monitoring and supporting the long-term sustainability of these stations.

1 Introduction

Space stations, once deployed, are designed to operate for decades [15]. The International Space Station (ISS) exemplifies this longevity, having supported scientific research for nearly 25 years. Today, a new generation of orbital habitats is emerging, including India's Bharatiya Antariksh Station [26], NASA's Lunar Gateway under the Artemis program [6], and Axiom Space's commercial modules [19]. Together, these platforms mark a new era of space infrastructure, with many designed to function autonomously and uncrewed for extended periods [12]. However, experience from the ISS has shown that long-duration missions demand consistent inspection and maintenance to ensure safety and reliability,

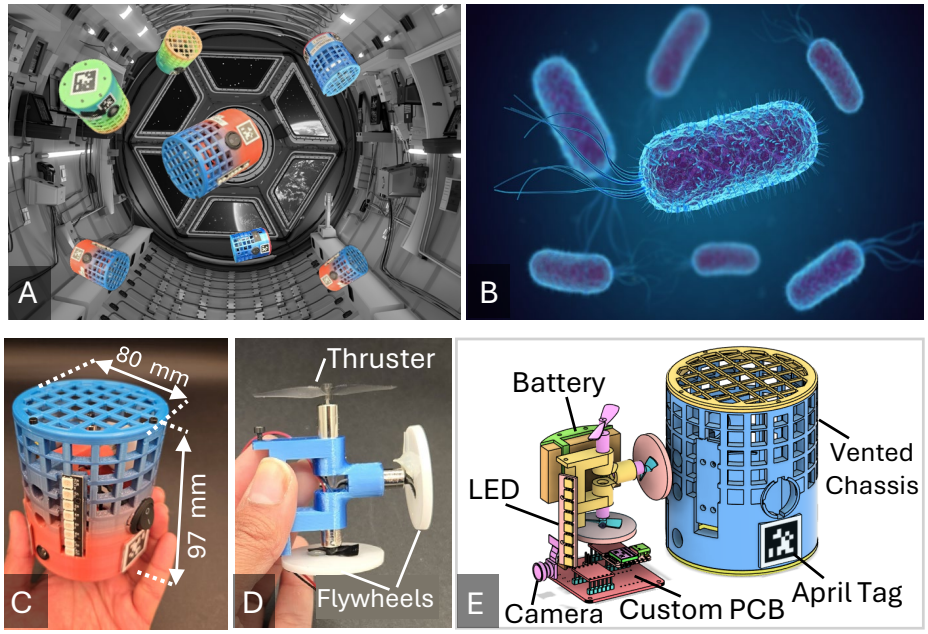

Robot	Size	Mass	# of actuators	Multi-Agent	Locomotion
SPHERES	20 cm	3.4 kg	12	Yes	Precise
Astrobee	32 cm x 32 cm	6.0 kg	14	Yes	Precise
Int-Ball	15 cm	1.0 kg	15	No	Precise
BFR	10 cm	0.2 kg	6	No	Precise
Tumblenauts	**8 cm x 10 cm**	**0.16 kg**	**3**	**Yes**	**Stochastic**

Fig. 1. *Tumblenauts* (A) Visualization of swarm operating inside a space station. (B) E. coli bacteria, the biological inspiration. (C) Robot dimensions. (D) Actuators: one thruster and two flywheels. (E) CAD model with labeled components. (Bottom Table) Comparison with other space robots: SPHERES[22], Astrobee[4], Int-Ball[23], BFR[17]

with recurring issues such as gas leaks often requiring complex human intervention [25]. This underscores a growing need for autonomous robotic systems [10] to monitor and maintain the structural health of space habitats.

In particular, free-flying robots designed for pressurized microgravity environments are emerging as powerful tools for intra-vehicular tasks within space stations. For example, NASA's Astrobee takes inventory and transports cargo [4], while JAXA's Int-Ball autonomously captures photo and video footage within the station [23]. Some of these robotic systems, such as NASA SPHERES [22] and NASA Astrobee [4], even demonstrate multi-robot coordination, working together to perform monitoring, inspection, and logistics tasks. Such cooperative systems are particularly effective for inspection, as they can operate in parallel, tolerate single-failures, and survey large areas with greater efficiency [28][20].

However, current single and multi-robot deployments are highly complex, incorporating numerous actuators and sophisticated control architectures in order to achieve extremely precise motions. This makes them energy-intensive, difficult to validate, and difficult to scale.

Meanwhile, in biological systems, we see a different paradigm. Bacterial swarms, for instance, move stochastically, drifting through spaces using run-and-tumble locomotion. They accomplish this form of random walk using a single flagellar actuator: during a "run", the bacterium's flagella rotate together to propel it forward, while during a "tumble", they reverse direction, causing the bacteria to randomly reorient [2]. Despite their remarkably simple actuation, stochastic motion combined with local interactions enables them to exhibit complex and intriguing emergent collective behaviors such as efficient exploration [29], gradient ascent [36], and quorum sensing [24]. Some engineered distributed systems also employ stochastic motion to operate efficiently in complex environments. For example, the ARGO float network in oceanography employs hundreds of minimally controlled drifting robots to provide long-term, high-frequency, global ocean observations—one of the most valuable sources of oceanographic data [30][5]. By leveraging stochasticity, each float has remarkable longevity, operating autonomously for three to five years on a single battery. Similarly, in microgravity, projects such as TESSERAE have investigated stochastic motion as a strategy for energy-efficient self-assembly of modular space habitats [11][31]. Here, free-flying tiles drift and interact stochastically until they connect, forming autonomous structures with minimal external control.

In this paper, we introduce the Tumblenaut, a minimalist, bacteria-inspired robot designed to autonomously inspect pressurized microgravity habitats, such as space stations, by leveraging collective behavior. Each robot moves stochastically, emulating the run-and-tumble locomotion of motile bacteria. By deliberately forgoing precise motion for stochastic behavior, we achieve a drastic reduction in mechanical complexity, making the Tumblenaut one of the smallest and least actuator-dense robots developed for microgravity. Moreover, the Tumblenauts are engineered for swarm deployment, emphasizing ease of manufacturing, scalability, and cooperative multi-robot functionality. This design philosophy is based on previous work in scalable swarm robotics [21][32][7], while extending to the unique constraints of microgravity.

The core contributions of this work are as follows. We present the design of the Tumblenauts (Sec 2.1) and experimentally characterize their run-and-tumble locomotion using Earth-based microgravity testbeds (Sec 2.2). Building on these results, we use a data-driven simulator to explore a family of collective behavior algorithms that demonstrate the autonomous inspection capabilities of the Tumblenauts (Sec 3). We show that these stochastically moving robots can (a) collectively build environmental maps (b) perform directed navigation by climbing both real and artificial potentials using a chemotaxis-inspired motion controller (c) make rapid and accurate environmental classification decisions using collective information sharing. Together, these results highlight the flexibility and capability of the Tumblenauts as a minimalist robotic platform for

intra-vehicular inspection. As a new generation of space habitats enters orbit, we envision swarms of Tumblenauts autonomously drifting through their interiors, providing scalable and resilient inspection for long-term space operations.

2 Design and Locomotion of the Tumblenauts

2.1 Robot Overview

A major design innovation of the Tumblenaut is its simple yet distinctive locomotion mechanism. Unlike most free-flying space robots, which depend on 6–12 actuators for full-state control (see table in Figure 1), the Tumblenaut achieves three-dimensional navigation with only three actuators by exploiting stochastic run-and-tumble motion. By deliberately trading precise position control for stochasticity, the Tumblenaut achieves a simpler, lighter, and more cost-effective design that scales well to large swarms.

Each Tumblenaut (Figure 1) weighs 160 g, measures 80 mm in diameter and 97 mm in height, and can be manufactured for approximately USD 50 per unit. The robot achieves run-and-tumble locomotion using commercial quadrotor components. The run motion is generated by a motor–propeller thruster identical to that used in Crazyflie drones [27]. Similar propulsion systems are employed in other free-flying space robots such as Int-Ball [23], Astrobee [4], and BFR [17]. The three-dimensional tumbling motion is achieved using two 35 mm acrylic flywheels mounted orthogonally, each driven by a quadrotor motor. The flywheels generate torque using angular momentum conservation, the same principle used for attitude control in satellites [33] and for locomotion in some planetary robots such as TorqueCapsules [39] and Hedgehog [14]. This turning mechanism is simple, eliminating the need for fluid interactions and relying solely on the rotation of internal masses. Critically, unlike previous free-flying robots that rely on sophisticated control architectures to maintain precise positioning and attitude, the Tumblenaut operates its actuators probabilistically, producing stochastic motion that reduces control complexity and enhances energy efficiency.

Each Tumblenaut is powered by a 3.7 V 1000 mAh Li-Po battery with USB and Qi wireless charging, and integrates a custom PCB featuring a XIAO ESP32S3-Sense microcontroller, dual DRV8833 motor drivers, OV2640 camera, MPU6050 IMU, SD card, and 8-LED Neopixel status strip. The robots communicate via ESP-NOW and can use AprilTags for local neighbor identification and relative positioning. All components are enclosed within a 3D-printed chassis for safe operation near humans or sensitive equipment.

2.2 Characterizing Run and Tumble Motion

We characterize the run-and-tumble dynamics of the Tumblenaut using Earth-based testbeds that partially emulate microgravity conditions. In particular, we (a) quantify the thrust generated during runs and (b) the angular velocity during tumbles. These measurements are used to refine the robot's design and to predict its dynamics in full microgravity using our data-driven simulator. Future work will involve verifying the robot's motion during a Zero-G flight.

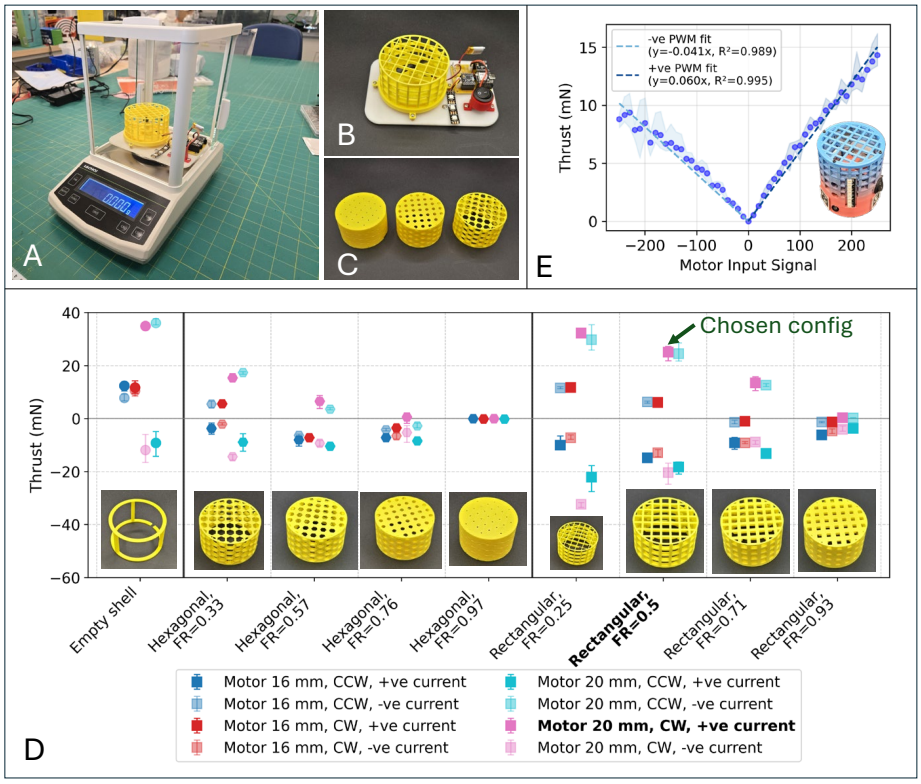

Fig. 2. *Thrust Characterization* (A) Precision scale for thrust measurement. (B) Rig for isolated thrust and venting tests. (C) Hexagonal vented chassis with varying fill ratios (FR). (D) Thrust test results comparing Bitcraze 16 mm and 20 mm motors, propeller directions (clockwise–CW, counterclockwise–CCW), and vent geometries. (E) Tumblenaut thrust vs. motor input signal (-255 to 255), where magnitude indicates power and sign indicates current polarity.

Characterizing Run To ensure safe operation near crew and sensitive equipment, all actuators in the Tumblenaut are enclosed within the chassis. This introduces complex fluid interactions, which we study by testing multiple venting and thruster configurations and using the results to refine the final Tumblenaut design. Thrust is then measured as a function of power, and secondary effects such as reaction torques are characterized. These results will inform run execution during upcoming Zero-G flights.

We measure thrust using a precision scale (Figure 2A), following standard procedures for drones and other free-flying robots [23]. We systematically tested different thruster types (16 mm and 20 mm Bitcraze motors), propeller orientations (clockwise and counterclockwise), and vented shell geometries (rectangular vs. hexagonal, varying fill ratios), as shown in Figures 2B–D. Rectangular vents with lower fill ratios produced greater thrust (Figure 2D). The 20 mm motor

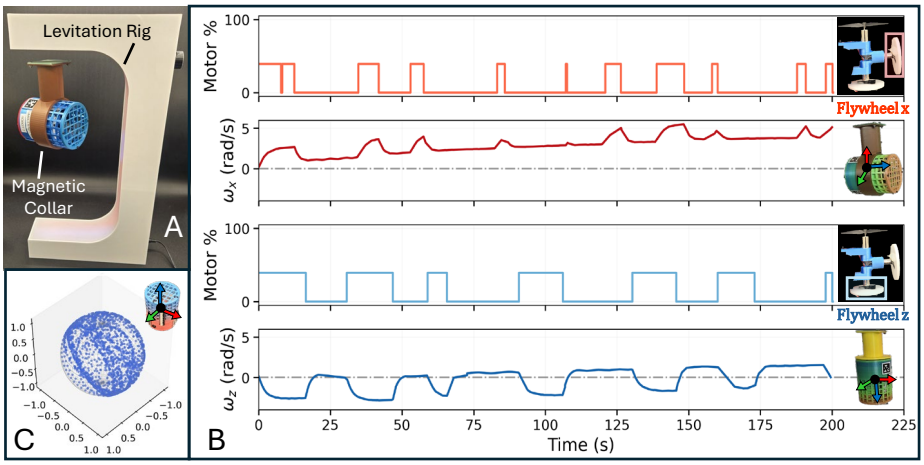

Fig. 3. *Tumbling Characterization* (A) Tumblenaut with magnetic collar suspended in the magnetic levitation system. (B) Flywheel motor input and corresponding measured angular velocities (ω_x, ω_z). (C) Thruster orientation over time reconstructed from the measured angular velocities in (B); red-x, green-y, blue-z axes.

outperformed the 16 mm version, with thrust direction determined by propeller orientation and current polarity. Based on these results, we selected a 20 mm motor with a clockwise propeller and a rectangular 0.5 fill-ratio venting pattern (8.5 mm vents) for the final Tumblenaut design, which offered a good balance between thrust efficiency and structural integrity.

We next analyze the relationship between thrust and power for the full Tumblenaut, which now includes internal components such as the flywheels and PCB (Figure 2E). Motor power is controlled via a motor input signal ranging from –255 to 255, with the magnitude and sign setting the power level and current direction. The Tumblenaut produces up to 14 mN of thrust, which is comparable to other free-flying robots of similar scale, such as Int-Ball (1.5 mN; [23]) and BFR (12 mN; [17]). A clear linear relationship is observed between thrust and motor power for both current polarities. Unlike the isolated thruster tests, where reversing the current reversed the thrust direction, the full Tumblenaut generates positive thrust regardless of current polarity. This effect is also observed in other enclosed-fan robots such as BFR [17] and Int-Ball [23].

We also observed that the thruster generates a reaction torque, causing the robot to spin when activated. This effect was verified by suspending the robot in a magnetic levitation system (described in the next section) and recording its angular velocity using the onboard IMU. At 70% power, the robot can achieve a rotational speed of up to 8.73 rad/s. To counteract this angular velocity, we implemented a PID controller that reverses the propeller's rotation, maintaining thrust in the same direction while producing an opposing torque. Each run cycle begins with positive current to propel the robot forward, followed by PID-

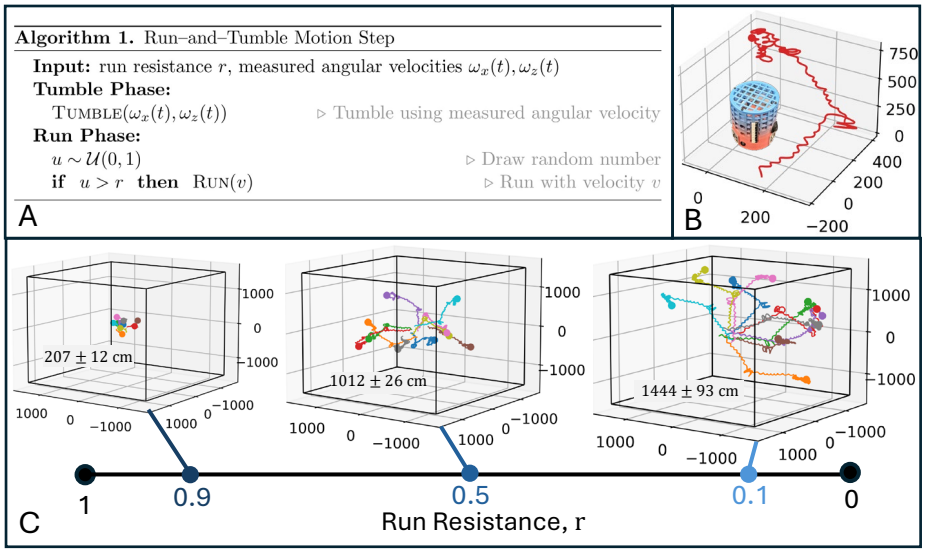

Fig. 4. *Run and Tumble Simulation* (A) Algorithm for a single run-and-tumble step. (B) Example Tumblenaut trajectory in the data-driven simulator. (C) 10 agent trajectories under varying run resistances; Text annotations in 3D figures show mean ± standard deviation of agent displacements from the origin over ten 100-s trials. All units are cm.

controlled counter-rotation to stop the robot from spinning (see supplementary video).

Characterizing Tumbling In this section, we analyze the tumbling dynamics of the Tumblenaut, ensuring that its orientation uniformly spans the full range of directions in three-dimensional space. Uniform tumbling is critical for effective exploration, as any directional bias would reduce spatial coverage.

To characterize tumbling, the Tumblenaut is fitted with a magnetic collar and suspended in a magnetic levitation system (Figure 3A and supplementary video). The magnetic field counteracts gravity, allowing the robot to rotate freely, replicating microgravity conditions along a single axis of rotation. Because the setup constrains motion to one axis at a time, we conduct two independent experiments measuring rotation about each flywheel axis (x and z). During each trial, the onboard IMU records angular velocity data, which is later combined in simulation to reconstruct the robot's full three-dimensional tumbling motion.

To achieve uniform tumbling, the two flywheel motors are toggled on (at 40% power) and off at random time intervals. Figure 3B presents a representative case of the two motor input signals and the resulting angular velocity outputs for each flywheel axis (x and z). Figure 3C plots the resulting orientation of the robot's z-axis, showing that it covers nearly the entire unit sphere. This confirms that the Tumblenaut tumbles relatively uniformly. A further advantage of this

stochastic control approach is improved energy efficiency, since the motors are only intermittently active rather than running continuously.

Run and Tumble Locomotion in a Data-Driven Simulator We now combine the experimental results from the previous sections to predict the run-and-tumble dynamics of the Tumblenaut in our data-driven simulator.

The Tumblenauts execute run-and-tumble motion by following the algorithm in Figure 4A. The robot is assumed to run at $v = 82$ cm/s when the thruster is active and remain stationary otherwise. This value, estimated from thrust measurements, corresponds to the terminal velocity at roughly 20% motor power. We assume the robot is tumbling according to the angular velocity measurements presented in Figure 3. We further add Gaussian noise with a standard deviation of 0.2 rad/s to simulate environmental perturbations and sensor variability. Figure 4B shows the trajectory of a single agent executing run-and-tumble motion. The current simulator is simplified, omitting key effects such as residual post-actuation velocity and assuming reflective boundary conditions. Future work will address these limitations using high-fidelity, physics-based simulators.

Tumblenauts can regulate their exploration dynamics by adjusting their run resistance r, which determines the probability that the thruster activates during motion. Figure 4C illustrates the exploration behavior of ten agents as run resistance is toggled. Robots with higher resistance remain close to their starting positions and explore less of the environment, whereas those with lower resistance travel farther and cover larger areas.

3 Leveraging Collective Behavior for Inspection

By leveraging collective behavior, the Tumblenauts serve as a powerful tool for intra-vehicular inspection. We highlight three ways stochastic swarm algorithms enable efficient inspection in microgravity. Using our data-driven simulator, we show that Tumblenauts can build measurement maps, navigate to regions of interest, and make inspection classification decisions (see supplementary video).

3.1 Collective Data Mapping

We consider a collective mapping task in which the Tumblenaut swarm measures and reconstructs spatial maps of environmental quantities such as temperature, pressure, or gas concentration. This capability is essential for monitoring the structural and environmental health of space stations, enabling early anomaly detection and supporting long-term maintenance [9]. This application parallels ocean mapping with ARGO floats [5], where large arrays of drifting sensors generate global maps without explicit coordination.

As an example, we task 10 randomly-positioned Tumblenauts with reconstructing the temperature field inside a confined, ISS-scale microgravity volume (1000m^3 [1]). Each robot independently performs run-and-tumble exploration with run resistance $r = 0.5$, logging temperature along its path. We assume the

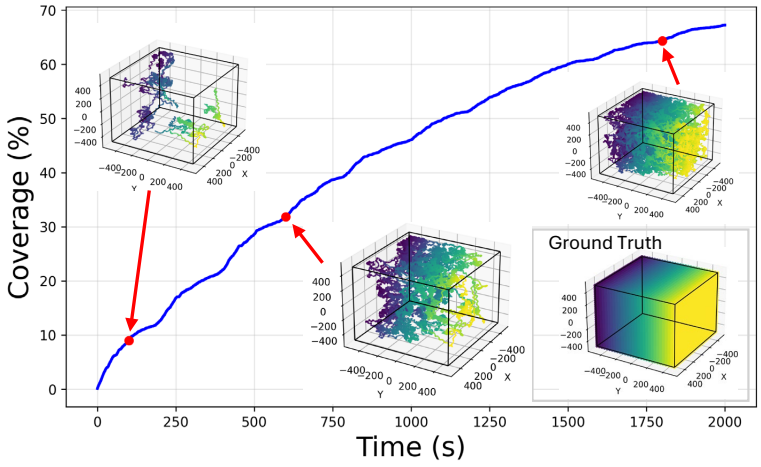

Fig. 5. *Collective Data Mapping.* Ten Tumblenauts map a 1000 m^3 environment (ISS-scale) under a linear potential. Insets show map progression over time; units in cm.

Tumblenauts have localization information and can upload data to a base station. The ground-truth temperature field is modeled as a simple linear gradient.

We evaluate mapping performance by measuring the swarm's spatial coverage over time (Figure 5), defined as the percentage of unique 20 cm voxels visited by the agents. Even with simple random motion and without coordination, the swarm collectively reconstructs the temperature distribution, producing a high-resolution thermal map. Across ten 2000-s trials, the swarm reconstructed an average of $64.6 \pm 2.7\%$ of the ground truth map. Future work will extend this preliminary demonstration to physics-based space-station environments and conduct sensitivity and parameter-tuning studies for deployment optimization.

3.2 Directed Navigation using Chemotaxis

Many long-duration inspection tasks require more control than purely stochastic motion. Inspired by bacterial chemotaxis [38][37], the Tumblenauts employ a Bacterial Chemotaxis Motion Controller (BCMC) to modulate their motion and climb local potential gradients to reach regions of interest. This enables purposeful navigation with stochastic motion.

The BCMC algorithm (Figure 6A) adjusts the run-resistance r based on whether locally sensed conditions are improving. We show that BCMC enables Tumblenauts to localize defects such as leaks: in Figure 6B, seven blue agents search for two gaussian leak sources using only local measurements of a normalized leak potential (e.g., air pressure). A leak is considered found when an agent enters within one standard deviation of the leak center ($\sigma_{leak} = 500$ cm). Even without a global map, inter-robot communication, or coordination, the agents find both leaks in all ten 400-s trials. In contrast, when the run resistance is fixed at $r = 0.1$, the swarm fails to find both leaks in any of the ten trials.

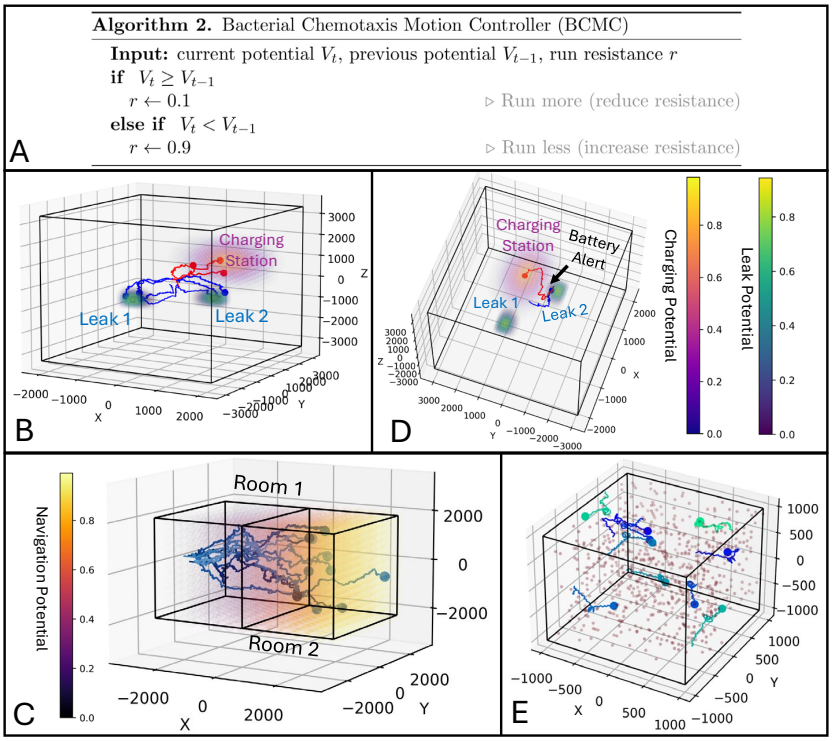

Fig. 6. *Directed Navigation and Environment Classification* (A) Single-step of BCMC algorithm showing how robots use potential measurements to adjust run resistance. (B) 7 blue agents climb a leak potential to locate leaks; 3 red agents follow a charging potential toward the charging station. (C) 10 agents navigate a linear potential to move across rooms. (D) An agent switches from climbing the leak potential to the charging potential upon getting a low-battery alert. (E) Ten agents using BayesBots to classify the environment as defective; red points denote defective voxels. All units in cm.

We can further generalize this to achieve a wide range of navigation goals by crafting artificial potentials. For example, an artificial Gaussian charging potential, $V = \exp\left(-\frac{\|p_{\text{agent}} - p_{\text{charge}}\|^2}{2{\sigma_{charge}}^2}\right)$, can attract agents toward a charging station, as seen by the red agents in Figure 6B. Here, p_{agent} and p_{charge} denote the agent and charging-station positions, and σ_{charge} controls the size of the charging region. Similarly, a linear navigation gradient can guide Tumblenauts between different rooms (Figure 6C). Moreover, these potentials can be dynamic. A robot might begin by following a leak-detection potential but, upon receiving a low-battery alert, switch to climbing a charging gradient instead (Figure 6D).

Therefore, with BCMC, the Tumblenauts can achieve many of the directed navigation capabilities of controllable space robots like Astrobee [4] and Int-Ball [23], while preserving the simplicity and energy efficiency of stochastic agents.

3.3 Classifying Environments using BayesBots Algorithm

Finally, we demonstrate that agents can leverage information sharing to make rapid and accurate decentralized inspection decisions, such as determining whether an environment requires maintenance. Specifically, we consider a scenario in which the robots must collectively decide whether the fraction of defective regions exceeds a critical threshold of 5%. A defective region may, for example, correspond to an area exhibiting abnormally high carbon concentration. A similar classification problem has previously been explored in two-dimensional settings [8][34], which we now extend to three dimensions.

In our setup, the environment is discretized into 1000 voxels (100 cm per side), each assigned a 10% probability of being defective (Figure 6E). We employ a Bayesian decision-making framework in which the robots perform random walks through the environment (run resistance $r = 0.5$), recording binary measurements that indicate whether sampled voxels are defective. Each robot accumulates its own observations and information received from neighbors until it reaches sufficient confidence to classify the environment. The swarm's performance is evaluated based on the proportion of robots that correctly identify the environment as requiring maintenance and the time taken to reach this decision.

We find that information sharing greatly improves collective decision-making, allowing the swarm to perform better than isolated agents. In experiments spanning ten runs with ten randomly-positioned agents, the communicating swarm achieved a mean classification accuracy of 0.960 ± 0.097 and a decision time of 60.7 ± 27.9 s. Without communication, accuracy dropped to 0.920 ± 0.042 and the mean decision time increased to 534.3 ± 3.89 s. Further details on the Bayesian formulation, parameter sensitivity, and optimization are provided in [34][35].

BayesBots represents one of many cooperative algorithms for inspection that the Tumblenauts can employ. The Tumblenauts can support a broad spectrum of additional collective approaches, including those detailed in [28][16][3][13][18].

4 Conclusion and Future work

We present the Tumblenauts, a bacteria-inspired swarm of microgravity robots that leverages collective, stochastic motion for intravehicular inspection. Future work will validate Tumblenaut locomotion in Zero-G flights, characterize inspection strategies in physics-based space-station simulators, and conduct user studies on Tumblenaut–astronaut cohabitation. Finally, due to their low cost, we envision Tumblenauts as an accessible educational platform for space robotics.

Acknowledgments. Funded by NSF CMMI-2036359 and an Amazon Robotics Research Award. Following [40], we report manually compiled gender citation rates: 22.2% W (first author)/W (last author), 22.2% M/W, 25.0% W/M, 30.6% M/M.

Disclosure of Interests. The authors have no competing interests to declare.

References

1. International Space Station Facts and Figures - NASA, https://www.nasa.gov/international-space-station/space-station-facts-and-figures/, section: Humans in Space
2. Berg, H.C.: Random Walks in Biology. Princeton University Press (Oct 2025), google-Books-ID: LAtYEQAAQBAJ
3. Berman, S., Halasz, A., Hsieh, M., Kumar, V.: Optimized Stochastic Policies for Task Allocation in Swarms of Robots. IEEE Transactions on Robotics **25**(4), 927–937 (Aug 2009). https://doi.org/10.1109/TRO.2009.2024997, http://ieeexplore.ieee.org/document/5161293/
4. Bualat, M., Barlow, J., Fong, T., Provencher, C., Smith, T.: Astrobee: Developing a free-flying robot for the international space station. In: AIAA SPACE 2015 conference and exposition. p. 4643 (2015)
5. Chu, W.U., Mazloff, M.R., Verdy, A., Purkey, S.G., Cornuelle, B.D.: Optimizing observational arrays for biogeochemistry in the tropical Pacific by estimating correlation lengths. Limnology and Oceanography: Methods **22**(11), 840–852 (2024). https://doi.org/10.1002/lom3.10641, https://onlinelibrary.wiley.com/doi/abs/10.1002/lom3.10641, _eprint: https://aslopubs.onlinelibrary.wiley.com/doi/pdf/10.1002/lom3.10641
6. Creech, S., Guidi, J., Elburn, D.: Artemis: An overview of nasa's activities to return humans to the moon. In: 2022 IEEE Aerospace Conference (AERO). pp. 1–7 (2022). https://doi.org/10.1109/AERO53065.2022.9843277
7. Dorigo, M.: SWARM-BOT: an experiment in swarm robotics. In: Proceedings 2005 IEEE Swarm Intelligence Symposium, 2005. SIS 2005. pp. 192–200 (Jun 2005). https://doi.org/10.1109/SIS.2005.1501622, https://ieeexplore.ieee.org/document/1501622
8. Ebert, J.T., Gauci, M., Mallmann-Trenn, F., Nagpal, R.: Bayes bots: collective Bayesian decision-making in decentralized robot swarms. In: International conference on robotics and automation (ICRA). pp. 7186–7192. IEEE (2020)
9. Ebert, J.T.: Distributed Decision-making Algorithms for Inspection by Autonomous Robot Collectives. Harvard University (2022)
10. Ekblaw, A., Coleman, C., Fish, S.: Into the ANTHROPOCOSMOS: A whole space catalog from the MIT Space Exploration Initiative. The MIT Press (2021)
11. Ekblaw, A., Paradiso, J.: Tesserae: Self-assembling shell structures for space exploration. Proceedings of the IASS Annual Symposia **2018**(1), 1–8 (2018), https://www.ingentaconnect.com/content/iass/piass/2018/00002018/00000001/art00007
12. Fuller, S., Lehnhardt, E., Zaid, C., Halloran, K.: Gateway program status and overview. Journal of Space Safety Engineering **9**(4), 625–628 (2022). https://doi.org/https://doi.org/10.1016/j.jsse.2022.07.008, https://www.sciencedirect.com/science/article/pii/S2468896722000763
13. Hauert, S., Winkler, L., Zufferey, J.C., Floreano, D.: Ant-based swarming with positionless micro air vehicles for communication relay. Swarm Intelligence **2**(2), 167–188 (Dec 2008). https://doi.org/10.1007/s11721-008-0013-5, https://doi.org/10.1007/s11721-008-0013-5
14. Hockman, B., Pavone, M.: Stochastic Motion Planning for Hopping Rovers on Small Solar System Bodies. In: Amato, N.M., Hager, G., Thomas, S., Torres-Torriti, M. (eds.) Robotics Research, vol. 10, pp. 877–893. Springer International Publishing, Cham (2020). https://doi.org/10.1007/978-3-030-28619-

4_60, http://link.springer.com/10.1007/978-3-030-28619-4_60, series Title: Springer Proceedings in Advanced Robotics
15. Jones, H., Hodgson, E., Kliss, M., Gentry, G.: How do lessons learned on the international space station (iss) help plan life support for mars? In: 46th International Conference on Environmental Systems. 46th International Conference on Environmental Systems (2016)
16. Leonard, N., Fiorelli, E.: Virtual leaders, artificial potentials and coordinated control of groups. In: Proceedings of the 40th IEEE Conference on Decision and Control (Cat. No.01CH37228). vol. 3, pp. 2968–2973 vol.3 (Dec 2001). https://doi.org/10.1109/CDC.2001.980728, https://ieeexplore.ieee.org/document/980728/
17. Liu, Y., Li, L., Li, H., Wang, X., Huang, Q., Ceccarelli, M.: A Compact and Low-Actuator Thrust System for Microgravity Flying Robot in Space Stations. IEEE Transactions on Industrial Electronics **72**(1), 629–638 (Jan 2025). https://doi.org/10.1109/TIE.2024.3401210, https://ieeexplore.ieee.org/document/10565905/
18. Lynch, N.A.: Distributed algorithms. Elsevier (1996)
19. Maender, C.: Beyond the iss: The world's first commercial space station. In: In-Space Manufacturing and Resources: Earth and Planetary Exploration Applications, chap. 17. Wiley (2022). https://doi.org/10.1002/9783527830909.ch17, https://onlinelibrary.wiley.com/doi/abs/10.1002/9783527830909.ch17
20. Mataric, M.J.: Designing emergent behaviors: from local interactions to collective intelligence. In: Proceedings of the second international conference on From animals to animats 2 : simulation of adaptive behavior: simulation of adaptive behavior. pp. 432–441. MIT Press, Cambridge, MA, USA (Aug 1993)
21. McLurkin, J.: Speaking Swarmish: Human-Robot Interface Design for Large Swarms of Autonomous Mobile Robots. AAAI spring symposium: to boldly go where no human-robot team has gone before (2006)
22. Miller, D., Saenz-Otero, A., Wertz, J., Chen, A., Berkowski, G., Brodel, C., Carlson, S., Carpenter, D., Chen, S., Cheng, S.: SPHERES: a testbed for long duration satellite formation flying in micro-gravity conditions. In: Proceedings of the AAS/AIAA space flight mechanics meeting. vol. 105, pp. 167–179. Clearwater, Florida, January (2000)
23. Mitani, S., Goto, M., Konomura, R., Shoji, Y., Hagiwara, K., Shigeto, S., Tanishima, N.: Int-Ball: Crew-Supportive Autonomous Mobile Camera Robot on ISS/JEM. In: 2019 IEEE Aerospace Conference. pp. 1–15 (Mar 2019). https://doi.org/10.1109/AERO.2019.8741689, https://ieeexplore.ieee.org/document/8741689/, iSSN: 1095-323X
24. Moreno-Gámez, S., Hochberg, M.E., van Doorn, G.S.: Quorum sensing as a mechanism to harness the wisdom of the crowds. Nature Communications **14**(1), 3415 (Jun 2023). https://doi.org/10.1038/s41467-023-37950-7, https://www.nature.com/articles/s41467-023-37950-7, publisher: Nature Publishing Group
25. NASA Office of Inspector General: Nasa's management of the international space station and efforts to commercialize low earth orbit (report no. ig-22-005). Inspection/Evaluation Report IG-22-005, National Aeronautics and Space Administration, Office of Inspector General, Washington, D.C., USA (Nov 2021), https://oig.nasa.gov/office-of-inspector-general-oig/ig-22-005/, issued November 30 2021
26. Phartiyal, B., Kumar, A., Shukla, S.: Martian/lunar analogue research station in india: Ladakh as a potential site. Current Science **128**(5), 10–03–2025 (2025), database: Academic Search Premier

27. Preiss, J.A., Honig, W., Sukhatme, G.S., Ayanian, N.: Crazyswarm: A large nano-quadcopter swarm. In: 2017 IEEE International Conference on Robotics and Automation (ICRA). pp. 3299–3304 (May 2017). https://doi.org/10.1109/ICRA.2017.7989376, https://ieeexplore.ieee.org/document/7989376/
28. Ramshanker, S., Ko, H., Nagpal, R.: Strategic Sacrifice: Self-Organized Robot Swarm Localization for Inspection Productivity. In: 17th International Symposium on Distributed Autonomous Robotic Systems (Nov 2024). https://doi.org/10.48550/arXiv.2411.09493, http://arxiv.org/abs/2411.09493, arXiv:2411.09493 [cs]
29. Rashid, S., Long, Z., Singh, S., Kohram, M., Vashistha, H., Navlakha, S., Salman, H., Oltvai, Z.N., Bar-Joseph, Z.: Adjustment in tumbling rates improves bacterial chemotaxis on obstacle-laden terrains. Proceedings of the National Academy of Sciences **116**(24), 11770–11775 (Jun 2019). https://doi.org/10.1073/pnas.1816315116, https://www.pnas.org/doi/full/10.1073/pnas.1816315116, publisher: Proceedings of the National Academy of Sciences
30. Riser, S., Freeland, H., Roemmich, D., et al.: Fifteen years of ocean observations with the global argo array. Nature Climate Change **6**, 145–153 (2016). https://doi.org/10.1038/nclimate2872, https://doi.org/10.1038/nclimate2872
31. Rollock, A., Pommier, M., O'Hara, W., Ekblaw, A.: Development of a Flight-Scale TESSERAE Habitat Concept for Biotechnology Research Outpost Applications. In: 2024 International Conference on Environmental Systems. 2024 International Conference on Environmental Systems (2024)
32. Rubenstein, M., Ahler, C., Nagpal, R.: Kilobot: A low cost scalable robot system for collective behaviors. In: 2012 IEEE International Conference on Robotics and Automation. pp. 3293–3298 (May 2012). https://doi.org/10.1109/ICRA.2012.6224638, https://ieeexplore.ieee.org/document/6224638/, iSSN: 1050-4729
33. Sidi, M.J.: Spacecraft Dynamics and Control: A Practical Engineering Approach. Cambridge Aerospace Series, Cambridge University Press, Cambridge (1997). https://doi.org/10.1017/CBO9780511815652, https://www.cambridge.org/core/books/spacecraft-dynamics-and-control/E9CAEE81CD09527C99497FA8C7C35B0A
34. Siemensma, T., Chiu, D., Ramshanker, S., Nagpal, R., Haghighat, B.: Collective Bayesian Decision-Making in a Swarm of Miniaturized Robots for Surface Inspection. In: Hamann, H., Dorigo, M., Pérez Cáceres, L., Reina, A., Kuckling, J., Kaiser, T.K., Soorati, M., Hasselmann, K., Buss, E. (eds.) Swarm Intelligence. pp. 57–70. Springer Nature Switzerland, Cham (2024). https://doi.org/10.1007/978-3-031-70932-6_5
35. Siemensma, T., Haghighat, B.: Optimization of Collective Bayesian Decision-Making in a Swarm of Miniaturized Vibration-Sensing Robots (Dec 2024). https://doi.org/10.48550/arXiv.2412.14646, http://arxiv.org/abs/2412.14646, arXiv:2412.14646 [cs]
36. Singh, S., Rashid, S., Navlakha, S., Bar-Joseph, Z.: Distributed Gradient Descent in Bacterial Food Search (2016)
37. Villa-Torrealba, A., Navia, S., Soto, R.: Kinetic modeling of the chemotactic process in run-and-tumble bacteria. Physical Review E **107**(3), 034605 (Mar 2023). https://doi.org/10.1103/PhysRevE.107.034605, https://link.aps.org/doi/10.1103/PhysRevE.107.034605

38. Wang, C.C., Ng, K.L., Chen, Y.C., Sheu, P.C., Tsai, J.J.: Simulation of Bacterial Chemotaxis by the Random Run and Tumble Model. In: 2011 IEEE 11th International Conference on Bioinformatics and Bioengineering. pp. 228–233 (Oct 2011). https://doi.org/10.1109/BIBE.2011.41, https://ieeexplore.ieee.org/document/6089832/
39. Yang, W.Y., Zou, Y., Huang, J., Abujaber, R., Nakagaki, K.: TorqueCapsules: Fully-Encapsulated Flywheel Actuation Modules for Designing and Prototyping Movement-Based and Kinesthetic Interaction. In: Proceedings of the 37th Annual ACM Symposium on User Interface Software and Technology. pp. 1–15. ACM, Pittsburgh PA USA (Oct 2024). https://doi.org/10.1145/3654777.3676364, https://dl.acm.org/doi/10.1145/3654777.3676364
40. Zurn, P., Bassett, D.S., Rust, N.C.: The Citation Diversity Statement: A Practice of Transparency, A Way of Life. Trends in Cognitive Sciences **24**(9), 669–672 (Sep 2020). https://doi.org/10.1016/j.tics.2020.06.009